Chalcogenide Letters Vol. 16, No. 4, April 2019, p. 175 - 184

EFFECTS OF Sn DOPING ON THE SEEBECK COEFFICIENT AND ELECTRICAL CONDUCTIVITY OF $Tl_9Sb_{1-x}Sn_xTe_6$ NANOPARTICLES

M. TUFAIL[a,*], W. H. SHAH[a], U. SHAH[a], W. M. KHAN[a], W. A. SYED[a], A. SAFEEN[b]

[a]*Department of Physics, Faculty of Basic and Applied Sciences, International Islamic University, H-10, Islamabad, Pakistan*

[b]*Department of Physics, University of Poonch, Rawalakot, AJK, Pakistan*

We report the effects of "Sn" doping on thermoelectric properties of thallium telluride $Tl_9Sb_{1-x}Sn_xTe_6$ (x=0.010, 0.025, 0.05) nano-particles, prepared by top down approach. Physically, all these compounds were found in phase as established by X-Rays (*XRD)* and energy dispersive x-rays spectroscopy investigation. The Seebeck co-efficient show increasing trends with rising temperature from 295 K to 550 K, further confirming p-type semiconductor characteristics. Multifaceted conduct of Seebeck coefficient for "Sn" doped compounds has been observed showing complex behaviour, Seebeck coefficient increasing with increasing contents from x= 0.01, 0.025 and 0.05.Similarly, the electrical conductivity (σ) and the power factors (PF) have also complex behaviour with "*Sn* "concentrations. The power factor observed for $Tl_9Sb_{1-x}Sn_xTe_6$compounds are increases with increase in the whole temperature range (295 K-550 K). Telluride's are narrow band-gap semiconductors, with all elements in common oxidation states, according to $(Tl^+)_9(Sb^{3+})$ $(Te^{2-})_6$,phases range were investigated and determined with different concentration of "*Sn* "with consequents effects on electrical and thermal properties.

(Received December 18, 2018; Accepted April 16, 2019)

Keywords: Sn doping, Sn doping effects on electrical and thermoelectric behaviour, Power factor optimization

1. Introduction

Energy storage and conversion devices continue to be rich areas for scientific and engineering studies that incorporate novel features and functions in intelligent and interactive modes, represent a radical advance in consumer products, such as wearable electronics, healthcare devices, artificial intelligence, electric vehicles, smart household, and space satellites. However, there are still grand challenges in fundamental research and understanding to accelerate energy storage and conversion devices to commercial reality, which include new materials and structures with high ionic conductivity, tailored mixed electron/ion conductivity, novel interface engineering methodologies, new device concepts, efficient and scalable techniques for materials and system-level integrations. This research study is intend to provide information's for those working in energy storage and conversion devices from materials, characterizations, devices and system integrations to communicate recent progress on current technologies and to exchange ideas about next-generation solutions.

The depleting situation of world-wide energy resources, different techniques of power generation including thermoelectric energy conversion has become increasingly significant [1].The efficiency of a thermoelectric (TE) power generator is determined from the properties of thermoelectric materials in terms of the dimensionless thermoelectric figure-of-merit, $ZT= S^2\sigma T/\kappa$ here S, σ,κ,T are Seebeck coefficient, electrical conductivity, thermal conductivity and the temperature, correspondingly. In over-all, σ increases with increasing carrier concentration while S is unevenly inversely proportional to carrier concentration. Term $S^2\sigma$ is recognised as Power factor (PF), it could be improved via carrier concentration. [2-4].

*Corresponding author: wiquar.hussain@iiu.edu.pk

Thermoelectric (TE's) materials with an extensive working temperature range for dissimilar quests in refrigeration and power generation have been widely considered [1, 14-17]. Thallium telluride (Tl_5Te_3) is one of the ultimate studied and used middle temperature TE materials with decent thermoelectric properties, appropriate for power generation applications.

The use of thermoelectric generator is determined by power factor (PF), measured by from square of Seebeck coefficient multiplied by electrical conductivity at specific temperature, that is $PF=S^2\sigma$.The power factor (PF)rest on considerably facts of the electronic band structure and carrier scattering procedure. The significant condition for attaining a large power factor (PF) is by means of maximizing Seebeck co-efficient S^2 and electrical conductivity σ. These conditions can be attained in materials, consuming complex band structure, high degree of degeneracy with numerous co-existing bonding kinds and scattering procedure. A collection of materials which gratify these necessities are the Sn doped ternary compounds of $Tl_9Sb_{1-x}Sn_xTe_6$. There is very confined data on the thermoelectric properties of Sn doped $Tl_9Sb_{1-x}Sn_xTe_6$nano-materials. Electrical, structural and thermoelectric properties of these compounds have been studied over temperature range 295 to 550 K as a purpose of unconventionality from stoichiometry.

To search the finest material for efficient thermoelectric generator, we must select the materials, which have high Seebeck effect and electrical conductivity. The lone material with decent thermal and electrical conductivity is metal, for the reason that their band gap is overlapped (continues energy states), but then again, their high thermal conductivity decreases the Seebeck co-efficient of the metals and brand it inappropriate for thermoelectric application, insulators which has an extensive band gap, because of which its electrical and thermal conductivities are low but not appropriate for thermoelectric application as a result of low electrical conductivity.

To develop high-performance nano-materials for thermoelectric generator, we have examined charge carriers inserted (Sn doped) thallium compounds as these kinds of nano-materials have tremendously low thermal conductivity as well as reasonable electrical performance as likened to their bulk corresponding item [18]. We have studied the properties of $Tl_9Sb_{1-x}Sn_xTe_6$ compound because of their low thermal conductivity [18] and high electrical conductivity and potential for their use as high efficiency bulk thermoelectric materials. To enhance the properties, these materials are characteristically doped to obtain charge carrier concentrations of the order of 10^{19}-10^{21} carriers per cubic centimetre. [19-21]. Weighty elements are recognised to donate to low thermal conductivity significant advantage of enhanced thermoelectric properties.

K. Kurosaki *et al*. [18] set the thallium antimony telluride $TlSbTe_2$ and inspected that the electrical resistivity is high and the thermal conductivity is low as likened to Sintered Bi_2Te_3 and TAGS "(GeTe)1-x($AgSbTe_2$)x" material. The Seebeck coefficient of $TlSbTe_2$ is 224 μVk^{-1} at 666 K which is positive in the entire temperature range displaying p-type behaviour. The power factor track for $TlSbTe_2$ is 8.9×10^{-4} $Wm^{-1}k^{-2}$ at 576 K which is low as likened the power factor of present thermoelectric devices i.e. in the range10^{-3} $Wm^{-1}k^{-2}$. Joseph P. Heremans*et al*. [22] uses the concept of electronic density of states to increase the power factor in Pb telluride PbTe, the Seebeck coefficient was improved through distorting the electronic density of states, principals to double the power factor and extra clarified that in nanostructure material it may bestow us more better-quality outcomes.

We have exposed materials with additional complex arrangements and structures that could give increase to high TE efficiency. TE materials necessitate are re-mixture of electrical and thermal properties, that is, challenge lies in attaining instantaneously high electrical conductivity σ, high TE power *S*, and low thermal conductivity k. All three of these properties are resolute by means of the facts of the electronic structure (band gap, band shape, and band degeneracy near the Fermi level, electronic concentrations) and sprinkling of charge carriers (electrons or holes) and therefore are not sovereign from to each other.

2. Experimental procedure

The Sn doped $Tl_9Sb_{1-x}Sn_xTe_6$ (x=0.01, 0.025, 0.05,) has been prepared through solid state reactions in evacuated sealed silica tubes. The determination of this study was largely for determining new kind of ternary and quaternary compounds by using Tl^{+1}, Sb^{+3}, $Sn^{+3}$and Te^{-}

[2]elements as the initial materials. Shortest synthesis of stoichiometric amount of high purity elements i.e. 99.99 % of unlike compositions have been prepared for an initial study. Since most of these preliminary materials used for solid state reactions are sensitive to oxygen and moistures, they are considering stoichiometric reactants and moving to the silica tubes in the glove box which is full of Argon. At that moment, all constituents were closed in a quartz tube. Earlier placing these samples in the resistance furnace for the heating, the silica tube was place in vacuum line to empty the argon and then closed it. This sealed power was heated up to 650 C° at a rate not beyond 1 k/mint and reserved at that temperature for 24 hours. The sample was cool down with tremendously slow rate to evade quenching, displacements, and crystals distortion. The nano-particles have been prepared by ball milling techniques with different size distribution [23].

Structural investigation of wholly these samples was carried out by means of x-rays diffraction, using an Intel powder diffractometery with position-sensitive detector and CuKα radiation at room temperature. No extra peaks were noticed in any of the sample deliberated here. X-ray powder diffraction patterns confirm the single-phase composition of the compounds.

The temperature dependence of Seebeck co-efficient was measured for all these compounds on a cold pressed pellet in rectangular form, of about 6x1x1 mm^3 dimensions. The air sensitivity of these samples was checked (for one sample) by measuring the thermoelectric power and established that these samples are not sensitive to air. This sample exposes to air more than a week, but no significant changes observed in the Seebeck values. The pellet for these measurements was annealed at 400 centigrade for 6 hours.

For the electrical transport measurements 4-probe resistivity method was used and the pellets were cut into rectangular form with estimated dimension of 6x1x1 mm^3.

3. Results and discussions

3.1. Structural analysis

X-ray diffraction is the best and significant method for the will investigation of crystal structure of dissimilar compounds, as well as for the approximate assessment of particle size using Debby Scherer's formula, and also with the purpose of to check the cleanliness of compound peaks in XRD data co-ordinated with the literature [22], as revealed in Fig. 1. It is authenticated that the XRD data for all these samples are found unchanging with and has been recognised that the crystal structure of the compound studied here are isostructural with reference data of Tl_9GdTe_6 and Tl_9BiTe_6 having tetragonal crystal structure with the space group symbol of Pb and a substitution variant of $Tl_{10}Te_6$ (Tl_5Te_3) [22, 30]. The crystal structure volume found for $Tl_9Sb_{0.99}Sn_{0.01}Te_6$ is 113.6, for $Tl_9Sb_{0.975}Sn_{0.025}T_6$ is 114.51 and for 115.6 for $Tl_9Sb_{0.950}Sn_{0.05}Te_6$. The crystallite sizes of the samples along with the lattice constant of the samples are given in table 1.

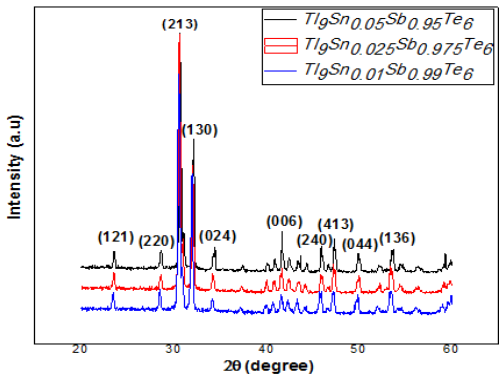

Fig. 1. XRD data of $Tl_9(SnSb)_1Te_6$ with Sn =0.01, 0.025 and 0.05, collected at room temperature.

Table 1. Crystallites size, Lattice constant & Volume.

Sample	Crystallites size "D"(nm)	Lattice constant $1/d^2= h^2+k^2/a^2+l^2/c^2$		Volume ($Å^3$)
$Tl^9Sb_{1-x}Sn_xTe_6$	0.9 λ/βcosθ	a=b	c	abc
$Tl_9Sb_{0.99}Sn_{0.01}Te_6$	31.8	8.82	12.88	113.6
$Tl_9Sb_{0.975}Sn_{0.025}T_6$	32.1	8.85	12.94	114.51
$Tl_9Sb_{0.950}Sn_{0.05}Te_6$	32.3	8.88	13.02	115.6

Powder X-ray analysis did not provide much information about the compositional analysis, shape and morphology of the nano-particles. For more details about the shape, surface and morphological analysis, we need energy dispersive X-ray spectroscopy (EDX) and scanning electron microscopy measurements.

3.2. Energy dispersive X-ray analysis

Energy Dispersive X-ray Analysis (EDX) has been used to investigate the qualitative and quantitative examination of the samples under investigation. EDX provides the information about the elements and their stoichiometry in the materials. Different elements will have different chemical shifts in the spectrum, which can be used as fingerprints. The sum of the areas under the peaks of each element is proportional to quantities in the material.

EDX spectrums of *Sn* doped nanoparticles in the $Tl_9Sb_{1-x}Sn_xTe_6$ with Sn=0.01, 0.025 and 0.05. From the spectrum, it has specified that the sample is weight percent (wt%) comprise of 1.10% Sn, 25.53%Te, 3.91% Sb and 69.46% Tl content in $Tl_9Sn_{0.01}Sb_{0.99}Te_6$ and the atomic percent (At%) sample is comprise of 1.59% *Sn*, 34.41% Te, 5.53% Sb and 58.47% Tl.

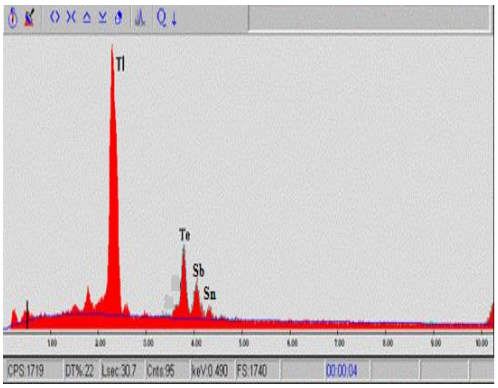

Fig. 2. Energy Dispersive X-ray Spectroscopy (EDX) of $Tl_9Sn_{0.01}Sb_{0.99}Te_6$ sample.

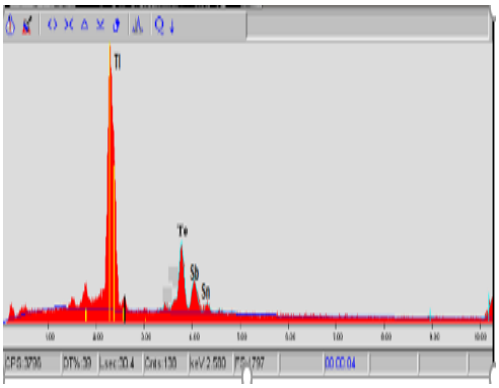

Fig. 3. Energy Dispersive X-Ray analysis image of $Tl_9Sn_{0.01}Sb_{0.99}Te_6$.

EDX spectrums of *Sn* nanoparticles doped in the $Tl_9Sb_{1-x}SnxTe_6$ with Sn=0.025. From the spectrum, it has specified that the sample weight percent (Wt%) comprise of 2.50% Sn, 25.60%Te, 2.82% Sb and 69.00% Tl content in $Tl_9Sn_{0.01}Sb_{0.99}Te_6$ and the sample is atomic percent (At%) comprise of 3.73% *Sn*, 34.41% Te, 34.41% Sb and 57.89% Thallium.

3.3. Scanning electron microscopy

SEM is generally used to investigate and examine phases, established on qualitative chemical evaluation of solid-state materials with its construction. This technique is also vital for qualitative or quantitative determination of chemical arrangements in samples through EDX spectroscopy and also used for determination of structure and orientations of crystals by using electron backscatter diffraction.

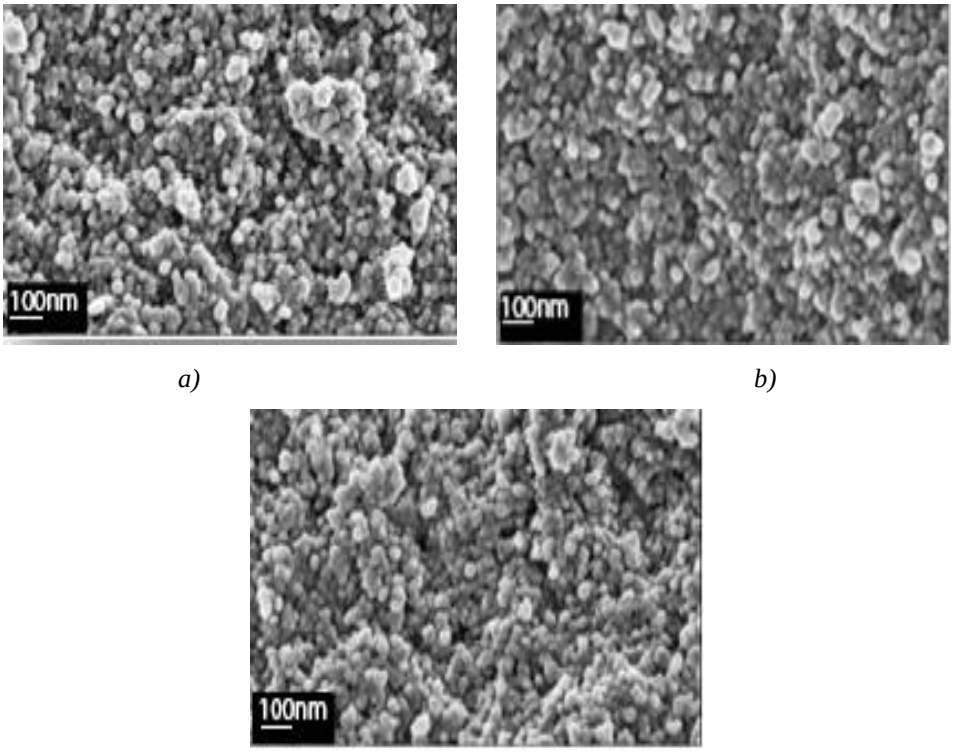

a) *b)*

c)

Fig. 4. $Tl_9 (SnSb)_1Te_6$ with SEM images of X =0.01 part (a), 0.025 part (b), and 0.05 part (c).

In Fig. 4, a, b and c images are the SEM images for the samples of $Tl_9Sb_{1-x}Sn_xTe_6$, x=0.01, 0.025 and 0.05 nano-structures with a bar scale of 100nm and with a high range of magnification, respectively.

The minor grain orientation by Sn concentration providing route for large electron scattering in $Tl_9Sb_{1-x}Sn_xTe_6$ for extra enhancement it is essential to elevating the materials at micro and nanometre levels which will improve thermopower.

3.4. Physical properties

3.4.1. Seebeck coefficient (S) measurements

The Seebeck coefficient of a material is also recognized as thermo-power which was concisely explained in Fig. 1.5. When the material's one side is being heated, the thermoelectric voltage increases due to thermal gradient, because charge carriers (electrons/holes) drift from the hot end to cold end [18]. The measurement of an induced voltage over a temperature gradient

$$S = \frac{\Delta V}{\Delta T} \tag{1}$$

between two sides of the material is known as See beck Coefficient, taking a seebeck coefficient into its component, it can be written as, the unit used for this coefficient is volt per Kelvin.

$$S = T\frac{8\pi^2 k_B^2 m^*}{3eh^2}\left(\frac{\pi}{3n}\right)^{2/3} \tag{2}$$

The equation is the See beck Coefficient for metals and degenerate semiconductors, in this equation there are three variables: the temperature, T, charge carrier concentration, n, and the effective mass, m^*. The power factor S is directly dependent on temperature and effective mass of the material, and inversely proportional to the carrier concentration of charges. The other terms in the equation are Boltzmann constant, k_B, electronic charge, $e = 1.67 \times 10^{-19}c$, and plank constant, $h = 6.626 \times 10^{-26}\text{k.g m}^2\text{sec}^{-1}$.

To examine the influence of decrease of the charge carriers in thermal and transport features, Sn was doped in $Tl_9Sb_{1-x}Sn_xTe_6$(x=0.01, 0.025 and 0.05) by means of replacing Sb atoms conferring to the formula. The temperature variation as a function of the Seebeck co-efficient (S) for the $Tl_9Sb_{1-x}Sn_xTe_6$(x=0.01, 0.025 and 0.05) nano-particles are revealed in Fig. 4. The See beck Coefficient was measured in the temperature gradient of 1 K. The positive See beck Co-efficient increases with increasing temperature from 295 K to 550 K, for all samples in mainly for p-type semiconductors having high charge carrier concentration. It is understandable that all the samples display positive Seebeck Coefficient for the whole temperature range, signifying that the p-type (hole) carrier's conduction controls the thermoelectric transportation in these types of nano-system. When the amount of Sn doping increased from 0.01 to 0.05, which supposed to increase the carrier's density in this type of materials configuration. Though, the smaller grains upon Sn doping are thought to be talented to improve the electron scattering, yielding an increase of the Seebeck co-efficient and effective mass [22-26]. It was found that only appropriate amount of Sn doping could advance the Seebeck co-efficient in this specific nano-system materials configuration. In additional, the Seebeck co-efficient will drop radically on doping from the optimum value of Sn concentration. More enhancements could be attained by means of (i) employing a fast fabrication process, for example melting spinning to decrease the grain size to a much greater degree, (ii) improving the doping elements and their consistent amounts to instantaneously enhance the charge mobility and carrier density to alongside improve the Seebeck co-efficient [25].

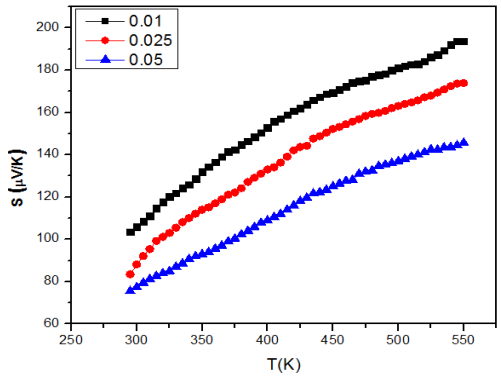

Fig. 5. Temperature dependence of Seebeck Co-efficient of $Tl_9Sb_{1-x}Sn_xTe_6$(x= 0.01, 0.025, 0.05).

3.4.2. Electrical conductivity

The temperature dependent electrical conductivity of the quaternary nano-systems is depicted in Fig. 5. The conductivity experiential for the entire samples are analysed here, decreases with increasing temperature, representing the degenerate semiconductor performance because of positive temperature co-efficient, subsequent from the phonons scattering of charge carriers and grains boundaries effects [27]. An increasing "*x"* value, (i.e. increasing the Sn deficiency) is predictable to increase the number of holes, which is experimentally detected. The smaller temperature need may be produced by (less temperature dependence) more grain boundary scattering. No systematic trend was found in the variation of the electrical resistivity for samples $Tl_9Sb_{1-x}Sn_xTe_6$(x=0.01, 0.025 and 0.05) with "Sn" concentration. The low electrical conductivity in the pressureless sintered sample [15-19] may be caused by means of the oxide impurity phase in the grain boundary and the number of the grain boundary. The *Sn* doping level and grain boundary resistance may play significant part for increasing electrical conductivity in these types of nano-materials.

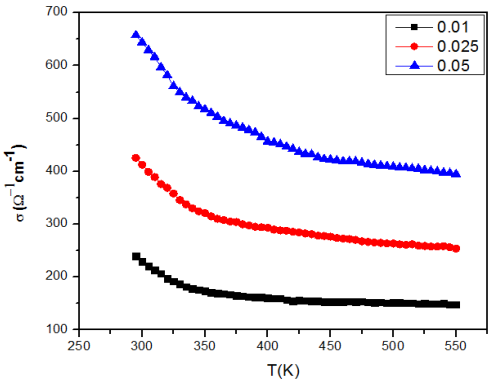

Fig. 6. Temperature dependence of electrical conductivity of $Tl_9Sb_{1-x}Sn_xTe6$ (x= 0.01, 0.025, 0.05) of the cooled pressed pellet, with heating profile.

The band structure calculations for $Tl_9Sb_1Te_6$ and $Tl_8Sn_2Te_6$ propose that $Tl_8Sn_2Te_6$ is a deeply doped p-type semiconductor with a partly unfilled valence band, though the Fermi-level E_f in $Tl_8Sn_2Te_6$ is situated in the band gap [5]. In consensus with these calculations, both thermal and electrical conductivity measurements specify that increasing Sn contents outcomes in lower values, as determined on sintered polycrystalline samples. For the Seebeck co-efficient, we have experiential an opposite trend increasing Sn concentration, reasons See beck values increases. The quaternary Nano-systems of electrical conductivity and mobility of electrons is also depending on the temperature. In metals, there is high temperature which will increases the vibration of phonons that affects the mobility of charge carriers and decreases the scattering time of electrons causing low electrical conductivity. In semiconductors high temperature increases the charge carrier concentration by moving of electrons from valence band to conduction band resulting good electrical conductivity. The exponential change i.e.

$$e^{-\frac{E_g}{2k_bT}} \tag{3}$$

occurs in the charge carrier concentration in intrinsic semiconductor.

The electrical conductivity 'σ' for the $Tl_9Sb_{1-x}Sn_xTe_6$ compounds with x=*0.01, 0.025 and 0.05* as depicted in Fig. 6 decreases with increase in temperature across the whole temperature range inspected here. These results are the revealing of metallic conductivity, an evidence of a comparatively high carrier concentration. Increased, doping concentration reasons decrease in "σ" as predictable and inversely affecting their Seebeck counterpart [20]. The sample with x= 0.05 i.e. $Tl_9Sb_{0.95}Sn_{0.05}Te_6$ displays the highest value of electrical conductivity i.e. 657.36(Ω-cm)$^{-1}$ at 295 K, and $Tl_9Sb_{0.99}Sn_{0.01}Te_6$discloses the lowest with 147.88(Ω-cm)$^{-1}$at 550K. The conductivity changes

at room temperature among the hot-pressed pellet and the ingot was observed a little alteration for the $Tl_9Sb_{0.975}Sn_{0.025}Te_6$sample.

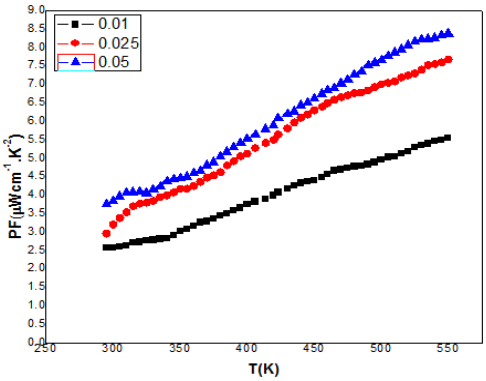

Fig. 7. Variation of Power factor with temperature and their dependency on doping Concentration for $Tl_9Sb_{1-x}Sn_xTe_6$(x=0.01, 0.025, 0.05)

To improve the power factor ($PF=S^2\sigma$) for these nano-system, we require to decouple the electrical conductivity from the Seebeck co-efficient, typically inversely proportional to each other. The key contribution in the 'PF' originates from the Seebeck co-efficient, so we must design the materials such that, their '*S'* should be improved. The power factors calculated from the electrical conductivity 'σ' and the square of Seebeck co-efficient 'S', gotten for $Tl_9Sb_{1-x}Sn_xTe_6$ nano-particles with x=0.01, 0.025 and 0.05 are showed in Fig. 8. The power factor increases with increasing temperature for all these samples. The doping concentration demonstrations a systematic effect on the power factor as increasing the doping concentration, the power factor is increases. The$Tl_9Sb_{0.95}Sn_{0.05}Te_6$compound showed the highest value 8.37(μWtt-cm^{-1}-K^{-2}) of "PF" at 550 K and 3.75(μWtt-cm^{-1}-K^{-2}) at 295 K. The lowest "PF" were experiential for $Tl_9Sb_{0.99}Sn_{0.01}Te_6$compound which have values of 5.55(μWatt-cm^{-1}-K^{-2}) at 550 K and 2.56(μWtt-cm^{-1}-K^{-2}) at 295 K. As deliberated earlier, an increasing the "Sn" contents are probable to increase the number of holes and the dominant charge carriers. This probable trend is experimental observed with increasing "x", the Seebeck co-efficient increases with *Sn* concentration, which results in increase in the "S". The smaller temperature dependence for some compounds may be produced by (less temperature dependence) additional grain boundary scattering. The ability of a material to conduct heat is thermal conductivity which is depend on the lattice vibration and number of free electrons in the material. In insulators the heat is transfers through phonons (lattice vibration) only, the total thermal conductivity is the contribution of lattice thermal conductivity κ_{ph} and electron thermal conductivity κ_e i.e.

$$\kappa = \kappa_e + \kappa_{ph} \tag{4}$$

In metals the free electron cloud is present, the heat is transfers through these free electrons and phonons, but the role of electrons in heat transfer is more than phonons. For metals the ratio of thermal conductivity to electrical conductivity is constant and known as Weidman-Franz law

$$LT = \frac{\kappa_e}{\sigma} \tag{5}$$

Where L is the Lorenz number and is given by

$$L = \frac{\pi^2}{3}\left(\frac{k}{e}\right)^2 \tag{6}$$

The Lorenz number depends on temperature depends on the temperature, position of the Fermi level and band structure of the material. For classical free electron model the Lorenz

number is $2.44\times10^{-8}[V^2K^{-2}]$, using the relation of Wiedemann-Franz law the thermoelectric figure of merit becomes

$$ZT = T \times \frac{S^2\sigma}{\kappa_e\left(1+\frac{\kappa_{ph}}{\kappa_e}\right)} \tag{7}$$

$$ZT = \frac{S^2}{L(1+\frac{\kappa_{ph}}{\kappa_e})} \tag{8}$$

This relation shows that the material with high thermoelectric figure of merit can be attained if the seebeck coefficient and electronic thermal conductivity (κ_e) is high and thermal conductivity of phonons (κ_{ph}) is low.

Debye also works on the conduction of heat by lattice vibration. In 1914 he theorized that in the case of elastic force between atoms the thermal conductivity should be infinite for a defect free crystal at all temperatures. The conductivity becomes finite if these forces are not same between the atoms. As a result the thermal conductivity also affected because it alter the sound velocity and scattering of the vibrational waves. The sound velocity is the velocity of sound waves in an environment. The Debye theory is further improved by Peierls by assuming that the kinetic theory of gases is valid for phonons and first time gives the concept of vibrational waves (phonons).

$$\kappa_{ph} = \frac{1}{3}C_v\nu l \tag{9}$$

$\kappa_{ph}$is the phonon thermal conductivity, C_v is the specific heat capacity, ν is the velocity of sound, l is the average distance before scattering travelled by vibration waves. The heat capacity can be found by the mean free path of the phonons because at high temperature ($T > \sim 300K$) the specific heat capacity and the velocity of sound are temperature independent. The other factors responsible or low thermal conductivity is the atomic disorder, large unit cells and the Debye temperatureθ_D, while θ_D is the temperature of the crystal's normal mode of vibration at which the phonons excited, it becomes small with low bond energies and high atomic masses, for heaver elementsθ_D is low while for lighter elements θ_D is high ranging from $38K$ for Cesium to $2230K$ for Carbon [20].

4. Conclusions

To understand our results, we start by final the basic understanding of the metallic long-range interactions, and semiconducting frustration effects foremost to metallic like conduct in these chalcogenide Nano-system. The structural examination exposed that $Tl_9Sb_{1-x}Sn_xTe_6$ single phase, all peaks are corresponding to their respective element and no additional peaks are experiential, which is conferring probable crystal structure for our project materials and demonstrations that there are no impurities or dislocation in the sample. EDS study confirms the percentage of elements existing in the sample studied here. The electrical characterizations show that parent compounds behave like a semiconductor, but increasing the *Sn* contents, these nano-materials tend in the direction of the induced metallic properties, which display that increasing the temperature the electrical conductivity will decreases at higher temperature.

The thermopower is positive in the whole temperature range studied here, which is increasing with increase in temperature, representing that the Nano-particles under study is hole conduction dominated. For higher concentrations of *Sn*, the Seebeck co-efficient of the doped tellurium telluride is decreasing because of increasing hole concentration which in turns increasing the electron scattering in this doped chalcogenide system. However, the smaller grains upon Sn concentrations will improve the electron scattering, resulting increase in thermopower. Therefore, power factor was improved and increased with high "Sn" concentration up to Sn=0.05 and the maximum power factor (PF=8.37 $\mu W cm^{-1}K^{-2}$) was observed for $Tl_9Sb_{0.95}Sn_{0.05}Te_6$. This enhanced

power factor will improve the thermoelectric efficiency and results decent thermoelectric applications, which is the key goal of this work. At the end, we are going to conclude that this study is the finest example of enhancing dopants concentration to attain required thermoelectric properties in "*Sn"*doped $Tl_9Sb_{1-x}Sn_xTe_6$ chalcogenide nano-system.

References

[1] T. Caillat, J. Fleurial, A. Borshchevsky, AIP conf. Proc. **420**, 1647 (1998).
[2] G. J. Snyder, E. S. Toberer, Complex thermoelectric materials. In Materials For Sustainable Energy: A Collection of Peer-Reviewed Research and Review Articles from Nature Publishing Group 101 (2011).
[3] H. Kleinke, Chemistry of Materials **22**(3), 604 (2009).
[4] M. G. Kanatzidis, Chemistry of Materials **22**(3), 648 (2009).
[5] B. C. Sales, B. C. Chakoumakos, D. Mandrus, Phys. Rev. B **61**, 2475 (2000).
[6] A. Harnwunggmoung, K. Kurosaki, H. Muta, S. Yamanka, Appl. Phys. Lett. **96**, 202107/1-3 (2010).
[7] K. Kurosaki, A. Kosuge, H. Muta, M. Uno, S. Yamanaka, Applied Phys. Letts. **87**, 061919/1-3 (2005).
[8] J. W. Sharp, B. C. Sales, D. G. Mandrus, B. C. Chakoumakos, Appl. Phys. Lett. **74**, 3794 (1999).
[9] S. Yamanaka, A. Kosuga, K. Kurosaki, J. Alloys Comp. **352**, 275 (2003).
[10] Q. Guo, M. Chan, B. A. Kuropatwa, H. Kleinke. Chem. Mater. **25**, 4097 (2013).
[11] B. Wolfing, C. Kloc, J. Teubner, E. Bucher, Phys. Rev. Lett. **86**, 4350 (2001).
[12] A. Kosuga, K. Kurosaki, H. Muta, S. Yamanaka, J. Appl. Phys. **99**, 063705/1-4 (2006).
[13] Q. Guo, A. Assoud. H. Kleinke, Adv. Energy Matter. **4**, 1400348/1-8 (2014).
[14] R. J. Campana, Adv. Ener. Conv. **2**, 303 (1962).
[15] R. J. Mehta, Y Zhang, C. Karthika etc., Nature Materials **11**, 233 (2012).
[16] G. S. Nolas, J. Poon, M. Kanatzidis, MRS, Bull 31199 (2006).
[17] B. A. Kuropaatawa, A. Assoud, H. Klienke, J. Alloys and Compounds **509**, 6768 (2011).
[18] K. Kurosaki, A. Kosuge, H. Muta, M. Uno, S. Yamanaka, Applied Phys. Letts. **87**, 061919 (2005); J. Yang, F. R. Stablers, J. Electrn. Mater. **3**(8), 1245 (2009).
[19] G. J. Synder, E. S. Toberer, Nat. Mater. **7**, 105 (2008).
[20] J. R. Soostsman, D. Y. Chung, Kanatzdis, M. G. Angew Chem. Inter. Ed. **48**, 8616 (2009).
[21] E. S. Toberer, A. F. May, G. J. Synder Chem. Mater. **22**, 624 (2010).
[22] Y. K. Kurosaki, Journal of Alloys and Compounds, p. 275, 2003, A. Pradel, J. C. Tedenac, D. Coquillat, G. Burn, Rev. Chim. Miner. **19**, 43 (1982).
[23] N. Rajput, International Journal of Advances in Engineering & Technology **7**(4), 1806 (2015).
[24] S. Y. Wang, G. J. Tan, W. J. Xie, G. Zheng, H. Li, J. H. Yang, X. F. Tang, J. Mater. Chem. **22**, 20943 (2012).
[25] H. Wang, A. D. Lalonde, Y. Pie, G. J Synder, Adv. Funct. Mater. **23**, 1586 (2013).
[26] Z. Cai, L. Guo, X. Xu, Y. Yan, K. Peng, G. Wang, X Zhou, J. Electronic Mater. **45**, 1441 (2016).
[27] K. T. Kim, T. S. Lim, G. H. Ha, Rev. Advanced Materials Science **28**, 196 (2011).
[28] H. Unuma, N. Shigetsuka, M. Takahashi, J. Mater. Sci. Lett. **17**, 1055 (1998).
[29] H. J. Goldsmid, J. W. Sharp, J. Electron. Mater. **28**, 869 (1999).
[30] K. F. Hsu, S. Loo, F. Guo, W Chen, J. S. Dyck, C. Uher, T. Hogan, E. K. Polychroniadis, M. G. Kanatzidis, Nature **489**, 414 (2012).
[31] Y. K. Kurosaki, Journal of Alloys and Compounds, 275 (2003).
[32] S. Bangarigadu-Sansay, C. R. Sankar, P. Schlender, H. Klienke, J. Alloys and Compounds **594**, 126 (2013).
[33] Wiqar H. Shah, Aqeel Khan, Waqas Khan, Waqar Adil Syed, Chalcogenide Letters **14**, 61 (2017).